

## WIND TUNNEL TEST OF A BLENDED WING BODY UNMANNED AERIAL VEHICLE

Raffaello Mariani<sup>1</sup>, Siwat Suewatanakul<sup>1</sup>, Sara Ghika<sup>1</sup>, Luis Alfonso Penela<sup>1</sup>, Per Wennhage<sup>1</sup> & Bin Zang<sup>2</sup>

<sup>1</sup>Department of Engineering Mechanics, Unit of Aeronautical and Vehicle Engineering, KTH Royal Institute of Technology, Stockholm, Sweden

<sup>2</sup>Department of Aerospace Engineering, University of Bristol, Bristol, UK

### Abstract

This paper discusses the wind tunnel test of a 37.5% scale model of a blended wing body unmanned aerial vehicle. The model was mounted on a fixed belly-fairing sting, and the pitch variation was facilitated via a linear actuator. The model and set-up were directly mounted on a force plate placed underneath the tunnel floor. Aerodynamic loads were acquired at a range of wind tunnel velocities between 10m/s and 30m/s, corresponding to a Reynolds number range between  $\sim 246\,000$  and  $\sim 760\,000$ , and results show good repeatability throughout the experimental campaign. A virtual wing tunnel was set up using computational fluid dynamics representative of the real-life facility, and the model was simulated inside the tunnel for a range of angles of attack between -4deg and 10deg without support, and at a reduced range between 0deg and 6deg with the support "installed." Classical analytical methods for boundary and support interference corrections were implemented, and correction factors were estimated by numerical simulation of the model with and without the support installed. Preliminary comparison between experimental measurements from force balance and numerical data show satisfactory agreement in the prediction of the lift curve slope, with some disagreement in the prediction of the stall condition. Prediction of drag and pitching moment are significantly impacted by the presence of the support and show poor agreement with numerical data.

**Keywords:** Wind Tunnel, Experimental Aerodynamics, UAV, Blended Wing Body

### 1. Introduction

A multidisciplinary research and educational effort towards sustainable aviation, called FLARE (Flying Laboratory for Aerospace Research and Education), has been recently initiated at the KTH, Royal Institute of Technology, encompassing all aspects related to developing the aircraft of the future, with the pilot project focusing on the development of a blended-wing-body (BWB) unmanned aerial vehicle (UAV) technology demonstrator powered by a compressed-hydrogen fuel-cell/Lithium-Ion system [1]. The objective of the project is to combine zero-net carbon offset propulsion with a highly efficient aircraft configuration such as a BWB [2] which has shown the potential for improvement in fuel consumption of up to 10% for typical mission of 6000nmi with a payload of 300 passengers [3], in an effort to address the issues of the aircraft of the future.

An integral part of any aircraft design process is the validation of the aircraft aerodynamic characteristics through experimental work in wind tunnel facilities [4]. The key aspects of for a successful wind tunnel test are geometric (model) and flow similarities (Reynolds number), the application of the appropriate boundary, in the case of testing in closed-jet wind tunnel, and support interference corrections [5]. These correction factors can be defined analytically, experimentally, or more recently through numerical simulation [6, 7].

The objective of the present work is to complete a wind tunnel test campaign of a 37.5% scale of a BWB UAV, starting from the preparatory work in a "virtual wind tunnel" for the definition of correction



Figure 1 – Wind Tunnel Model

factors and the validation of these corrections as applied to experimental data, to the analysis of the aerodynamics of the aircraft to gain further knowledge with respect to performance. The objective is reflected in the structure of the paper. Section 2 presents the experimental set up and methodology. Section 3 and Section 4 discuss the methodology for data correction through the implementation of a (numerical) “virtual” wind tunnel, followed by the discussion in Section 5 of the validation of the correction methodology and parameters applied to experimental data. Aerodynamic performance is presented in Section 6. Future Work and Conclusions are presented in Section 7 and Section 8, respectively.

## 2. Experimental Set Up

### 2.1 Wind Tunnel

Tests were conducted in the closed-circuit, closed-jet Large Low-Speed Wind Tunnel at the University of Bristol. The test-section has an octagonal cross-section of 7ft-by-5ft (2.1m-by-1.5m), approximately 3m in length and it can attain a maximum wind speed of 60m/s. The wind tunnel is equipped with a 6-components force plate (OPTIMA Biomechanics Measurement Systems BMS400600) placed underneath the tunnel floor. Tests were conducted at a range of wind tunnel speeds between 10m/s and 30m/s, with the reference condition being 30m/s.

### 2.2 Wind Tunnel Model

The model has a wingspan of 1.5m [8], and it was sized to have an overall blockage of less than 5%. The model has a core structure in the fuselage composed of an aluminium plate and ribs for assembly with the support and actuator, an internal structure in the wings composed of carbon composites rods and PET/Carbon fiber sandwich ribs and spars, and carbon fiber skins. The model is also equipped with 64 pressure taps on the left-hand side of the fuselage section, with mounting plates for the scanivalves manufactured with PLA based 3D printing. The model in preparation and the full assembly in the tunnel are shown in Figure 1.

### 2.3 Model Support and Pitch Angle Actuator

A dedicated support [9] was designed and manufactured for the test. The support is composed of an aluminium flat plate that mounts directly onto the force plate, a 40mm-diameter steel sting welded to a circular base plate free to rotate, and a locking ring to secure the rotating plate and sting, and set to the desired yaw angle. The pitch-angle motion of the aircraft is controlled by a rear-mounted linear actuator from Firgelli Automations (Model FA-OS-400-12-24), equipped with an optical sensor position feedback, 400lbf (1790N) push/pull, 24in stroke (609mm), remotely controlled through MATLAB Symulink. Mechanical rotation was assured through clevis mounts. Position feedback was ensured using a WITMOTION attitude sensor installed inside the model.

### 2.4 Assembly and Model Positioning

As mentioned in Section 2 the model was mounted on a force plate placed underneath the tunnel floor. The force balance was oriented as shown in Figure 3 with the positive  $y_b$  axis pointing upstream

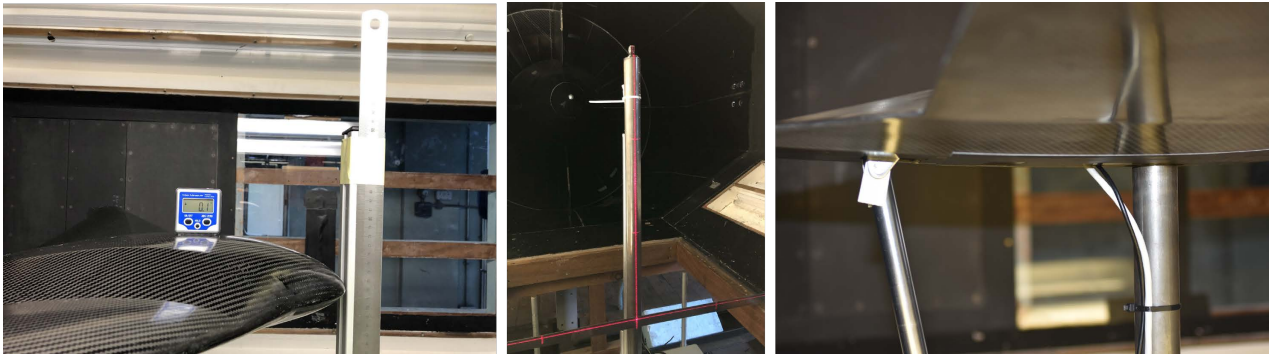


Figure 2 – Wind Tunnel Assembly and Positioning

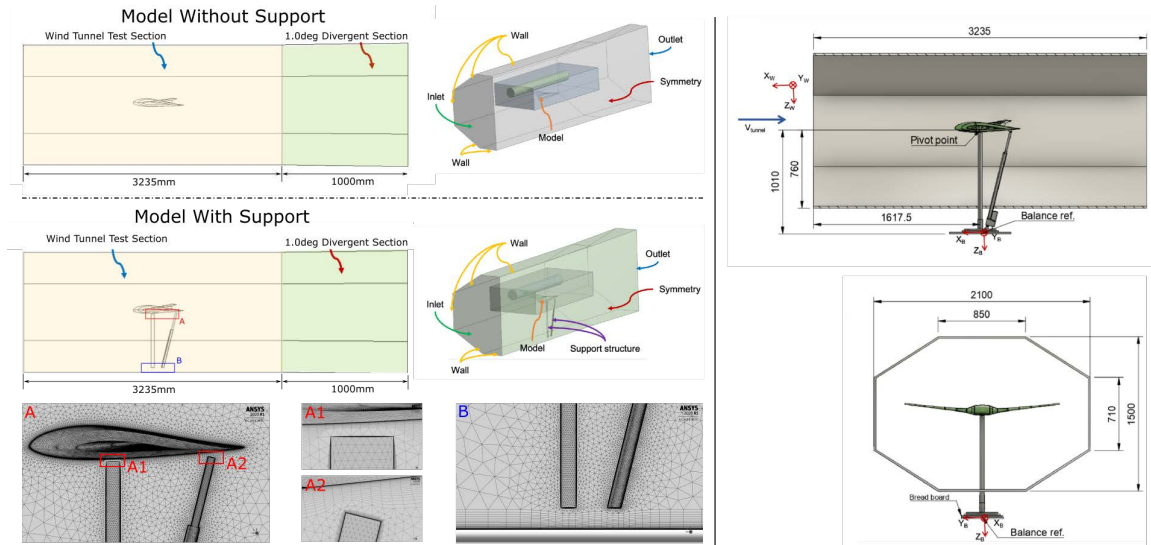


Figure 3 – Virtual Wind Tunnel Computational Domain [10]

in the direction opposite to the flow, the positive  $x_b$  pointing outboard of the left wing, and the positive  $z_b$  pointing downwards in a classical “right-hand-rule” orientation. Alignment of the support and leveling of the model was completed using a laser level, and the zero angle of attack was verified with an external digital inclinometer prior to zeroing the internal inclinometer and the feedback signal of the rear actuator. Cables for the instrumentation placed inside the model were routed along the belly-fairing stream (downstream face) for minimal interference. The assembly is shown in Figure 2.

### 3. Virtual Wind Tunnel Set Up

A “virtual wind tunnel” geometrically consistent with the experimental facility was implemented to complete preparatory work for the wing tunnel testing, particularly with the objective of validating blockage and wall correction, and of determining the coefficient for support interference corrections [11]. A computational domain consistent with the experimental facility was constructed using Ansys Fluent tools. The octagonal cross section has a maximum width of 2100mm and a height of 1500mm, and a length 3235mm, with the model placed at the centre of the test section, as shown in Figure 3. A 1.6m-long, 1.0deg divergent section was added at the outlet of the test section to improve convergence.

Two cases were simulated: model without the support structure; and model with the support structure. For the case of model with support, the geometry was simplified for computational reasons by removing the connecting geometry between support and model and support and floor, as shown in Fig. 3 (magnified sections A and B), effectively introducing a small gap between the structures.

The surface mesh of the aircraft model was separated in two parts: main body and wing section with an element size in the order of  $5 \times 10^{-3}$ ; and the wing tip section with an element size in the order of

$1 \times 10^{-3}$ . Hexahedral inflation layers from the model were created to achieve a target of  $y^+ = 1$ , with a corresponding first layer thickness  $\Delta_s = 7.5 \times 10^{-6}$  with a growth factor of 1.15 and a maximum number of layers of 42 [10]. A similar approach was used along the walls of the wind tunnel. A tetrahedral unstructured mesh filled the volume of the computational domain. The number of elements for each case is listed in Table 1.

| Case            | Number of Elements |
|-----------------|--------------------|
| Without Support | 3.1 million        |
| With Support    | 3.5 million        |

Table 1 – Mesh Elements

Simulations were conducted using steady-state Reynolds Averaged Navier Stokes (RANS) equations with applied energy equation, coupled with a  $k - \omega$  SST turbulence model as it is widely used in aeronautical applications [11]. A pressure-based solver was used coupled with the second-order discretization scheme as it provides a robust and efficient application. Inlet velocity was set to 30m/s to represent the reference wind tunnel velocity, with flow conditions set at standard sea-level values. Turbulence intensity for the facility was not know and was therefore assumed at a value of 1% [12].

## 4. Boundary and Support Interference Corrections

### 4.1 Methodology

In order to correctly compare experimental and “flight” data, boundary and support interference corrections need to be applied to force balance data. These corrections have traditionally been calculated analytically through classical approaches [13], although more recently numerical simulations of testing conditions have been implemented, particularly for support interference [6, 7] in order to determine correction factors ahead of the tests.

In the current study, for solid and wake blockage, which primarily affect the dynamic pressure and therefore the coefficients of lift and drag in primis, classical methods have been applied [13] and validated initially using numerical data of the “free flight” and virtual wind tunnel case of model with no support for a range of angles of attack between -4deg and 10deg, effectively capturing the stall region of the aircraft.

Support interference corrections were determined solely using numerical simulations, at a reduced range of angles of attack between 0deg and 6deg. Lift, drag, and pitching moment were obtained for the model with and without support support case, alongside aerodynamic loads from “free flight.” The approach of “ $\Delta$ -Calculations” [14] was implemented, where data from free flight and from the virtual wind tunnel case without support is subtracted from data obtained by simulations obtained with the support, for which a generic case for lift is shown in Equation 1 as an example:

$$\Delta L_{x_{flight,WT}} = L_{x_{flight}} - L_{x_{WT_{wb}}} \quad (1)$$

where the subscript *WT* represents wind tunnel data (numerical or experimental) and the subscript *wb* means corrected for blockage. These values are then plotted as a function of angle of attack and correction factors are obtained by applying a second-order polynomial curve fit, as shown in Equation 2.

$$\Delta L_c(\alpha) = A\alpha^2 + B\alpha + C \quad (2)$$

where the subscript *cf* is for “correction”, and *A*, *B*, and *C* represent the corrections factors as a function of angle of attack  $\alpha$ . The correction value is then subtracted from the reference data to obtain the final aerodynamic loads, as shown in Equation 3 for the example case of lift.

$$L_{corrected} = L_{flight} - \Delta L_c \quad (3)$$



### 4.2 Validation of Methodology

The first step in the validation of the correction focused on solid and wake blockage [13], which resulted in a total blockage  $\varepsilon_t = 0.0027$  for a corrected dynamic pressure at the reference wind speed of 30m/s of  $554.2N/m^2$ , or a correction of 0.5% with respect to “free flight” conditions [10].

Reference “free flight” data is initially compared with uncorrected data and with data corrected for blockage for “virtual wind tunnel” case without support [10]. These results indicate that blockage effects are negligible for angles of attack where flow is fully attached, with a small departure as flow begins to separate beyond  $\alpha = 6deg$ . The difference between reference the corrected “virtual wind tunnel” data for the case of the model in the tunnel without support is in the range of 0.2% to 0.5% for lift and drag, and of 2% for pitching moment coefficient, as shown in Figure 4.

Reference “free flight” data is subsequently compared with uncorrected and fully corrected data of the “virtual wind tunnel” case of model with support [10]. Results show that the presence of the support has a stronger impact on the flow around the aircraft, and therefore on the predicted aerodynamics loads. As shown in Figure 5, the flow over the upper surface remains mostly unchanged, except for minor effect at higher angles of attack due to flow separation. The pressure distribution over the lower surface is affected differently from the ase without support as the angle of attack is increased due to the wake of the support more closely interacting with the flow over the lower surface.

As shown in Figure 4, the variation in pressure distribution results in a shift towards the right (i.e. “seeing” higher angles of attack) of the lift and pitching moment curves with respect to angle of attack while the curve slopes remain mostly unaffected. On the other hand, the drag curve with respect to angle of attack is affected both in orientation and, as expected, in terms of an increase in drag values. As can be seen in Figure 4, the methodology discussed in Section 4.1for taking into consideration the effects of the support interference provides satisfactory results, in particular in terms of lift and drag coefficients. Lift coefficient data corrected for support inference departs from the corrected data of the case of the model in the wind tunnel without support and from reference “free flight” data by  $\sim |1\%|$  and by  $\sim |5\%|$ , respectively. Agreement between reference and fully corrected data, and wind tunnel without support and fully corrected data including support interference, is in the range of  $\sim |3\%|$ . These values are considered satisfactory for preliminary work.

With regards to the corrections of the pitching moment coefficient, support interference corrections are effective at small angles of attack, with differences in excess of  $\sim |10\%|$  beyond  $\alpha > 4deg$ . At higher angles of attack, where the flow begins to separate and becomes unsteady, wake flow is modelled as “mean flow,” which results in a less accurate mapping of the pressure distribution over the wing, which ultimately has a significant impact on pitching moment, much more so than on lift and drag coefficients.

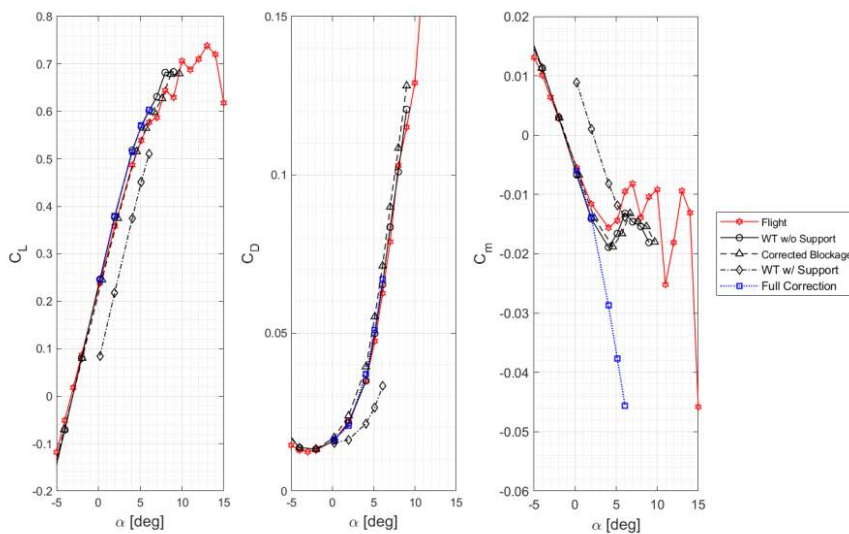


Figure 4 – Reference Numerical Data vs. Virtual Wind Tunnel Data [10]

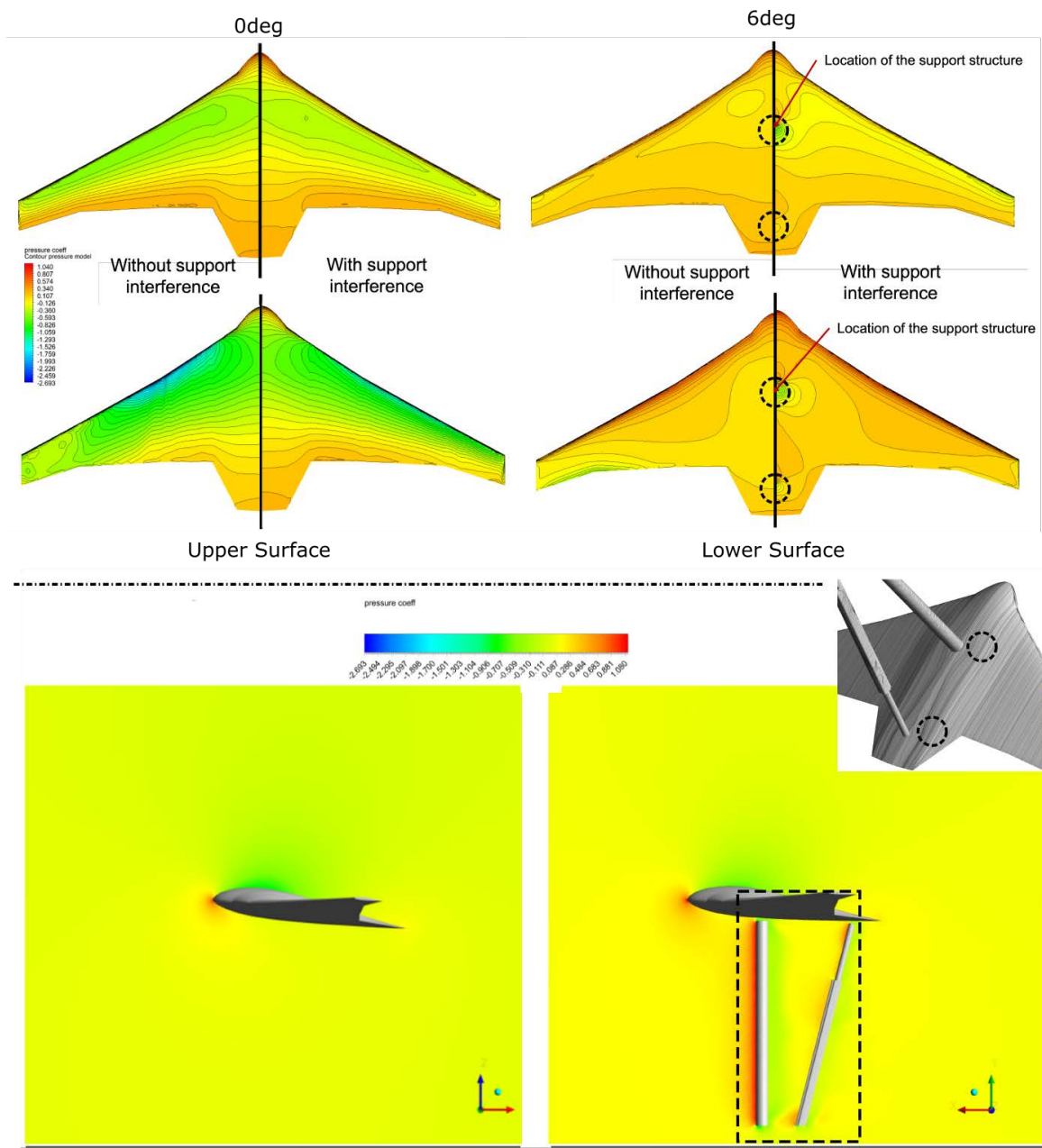


Figure 5 – Pressure Distribution of Flow With and Without Support [10]

## 5. Wind Tunnel Test Preparation and Validation

### 5.1 Opening of the Experimental Domain

A “shake down” of the set up opened the experimental campaign, by progressively increasing the wing speed from 10m/s to 30m/s, corresponding to a range Reynolds number range between  $\sim 246\ 000$  and  $\sim 760\ 000$ , to determine Reynolds numbers, conscious of the fact that the flight Reynolds number of  $\sim 1\ 300\ 000$  could not be attained as it corresponded to a tunnel velocity of  $\sim 50\text{m/s}$ , which was deemed to high for these preliminary tests.

In addition, “the shake down” helped to validate the ability to correctly position the aircraft under increasing aerodynamic loads. The “shake down” did not highlight any particular issues with the set-up, e.g. excessive vibration at stall, indicating that tests could be safely carried out at a wind speed of 30m/s. At the same time, the small vibration of the model due to flow separation caused some minor inconsistencies in the readings of the actuator feedback data compared to the internal inclinometer, and therefore resulted in some outlier data points in the curves, as shown in Figure 6.

Uncorrected lift and drag data at wind velocities between 10m/s and 30m/s are shown in Figure 6 (left). Data show that the linear section of the lift curve is only marginally affected by the velocity

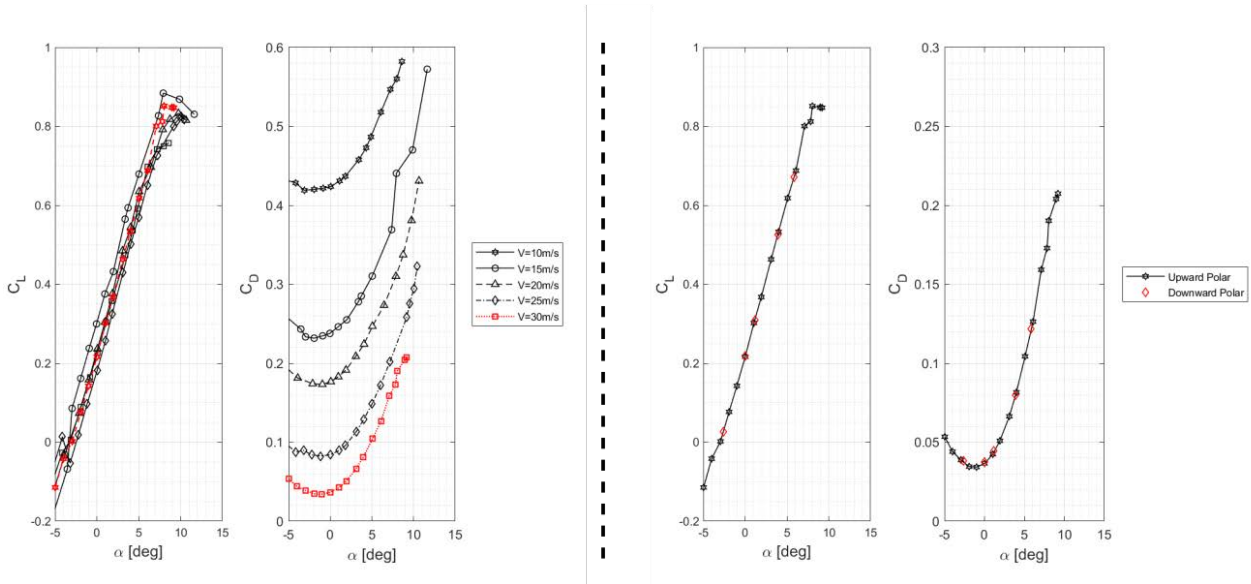


Figure 6 – Opening of the Testing Domain (left) and Repeatability (right)

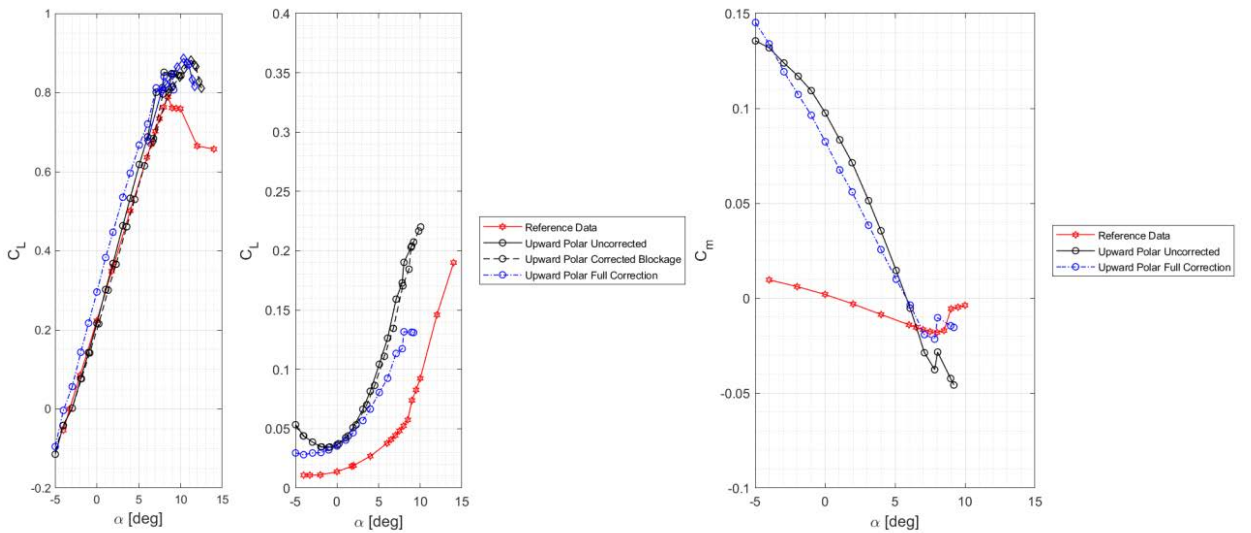


Figure 7 – Reference [1] vs. Wind Tunnel Data

variation, which is to be expected, with more variability present in the stall region as flow separation is highly affected by variations in Reynolds number. As expected, drag coefficient is highly affected by Reynolds number effects. As a matter of fact, maximum lift coefficient is steadily increasing with increasing Reynolds number, with the outlier of data at  $V=15\text{m/s}$ .

Repeatability was assessed by acquiring data points at known angles of attack in a downward polar at the reference velocity of  $30\text{m/s}$ . Results in Figure 6 (right) show good short term repeatability, as indicated for example Agreement at  $\alpha = 0\text{deg}$ , for example, is  $\sim 1\%$ .

### 5.2 Validation of Wind Tunnel Corrections

Blockage and support interference corrections obtained from the virtual wind tunnel simulations were applied to experimental data, and the comparison is shown in Fig. 7.

As shown qualitatively, there do not seem to occur significant differences between reference data [1], uncorrected data, and data corrected for blockage and wall effects in the linear portion of the lift curve. A quantitative comparison between  $-2\text{deg} \leq \alpha \leq 6.5\text{deg}$  indicates an average difference of  $\sim |2\%|$ , which may be considered an acceptable discrepancy between numerical and experimental data. Similar results were observed for the drag coefficient.

The consistency of uncorrected data and data corrected for blockage with respect to reference data means that, once corrected for support interference, the lift curve is shifted towards the left as expected from the results of the “virtual wind tunnel”, although in this case resulting in an overprediction of the lift coefficient. Corrections for drag are more consistent as its magnitude is generally reduced compared to uncorrected data, although results indicate that the corrections factors may not be “sufficiently strong” to be applied directly to the experimental data. Stall conditions do not appear to be affected by the corrections.

Pitching moment curves show a non-negligible disagreement between uncorrected and corrected data, and a significant departure from reference data. The differences between reference and experimental wind tunnel data will be discussed more in detail in Section 6.

Results from these opening tests confirmed the feasibility of testing at 30m/s as the design test velocity, and that good repeatability is achievable with the current set-up. Data also confirms that blockage is not an issue for the experiment, and that preliminary support interference corrections may be considered acceptable for lift and drag.

## 6. Aerodynamic Results

The full analysis of the aerodynamic performance of the aircraft was conducted at the reference wind speed of 30m/s. Fully corrected data, which also includes corrections for dead-weight, will be discussed with respect to numerical reference data (where applicable), including a preliminary qualitative assessment of the coefficient of side force, roll and yaw moment.

The analysis of the aerodynamic performance of the aircraft is shown in Figure 8 for all six components. Lift, drag, and pitching moment coefficients are compared with reference numerical data, while side force, roll and yawing moment are only available experimentally and are therefore mostly indicative of any issue in model or set-up alignment. Reference data is taken from Suewatanakul et al. [1].

Drag is over predicted in the experimental campaign compared to the reference numerical data, as can be seen, for example, at  $\alpha = 0deg$ , where drag “jumps” from  $0.0138$  for the reference case to  $0.0373$  for the experimental case. In the experimental environment, part of this discrepancy can be attributed to quality of the surface finishing of the model, as it is known to have a non-negligible impact on the measurement of drag, and in part to the added drag caused by the support interference, which has been shown in Section 5 to be insufficiently corrected. In the numerical RANS simulation, the mesh refinement at the surface, and particularly the choice of the boundary conditions have a significant impact on the accuracy of prediction of drag, which in turn may be under estimated. In addition, the turbulence intensity is not known, introducing an extra level of uncertainty in the comparison of the data.

Results show that both uncorrected data and data corrected for blockage agree well with reference data, which is in some respects unexpected as support interference should still have a non-negligible impact on the measurements. When corrected for support interference, the lift curve is shifted to the left, as expected from the discussion in Section 4, resulting in an overestimation of performance and a shift in slope of the lift curve. In addition, experimental data show the distinct trend of over-predicting the maximum lift coefficient by  $\sim 10\%$  as well as the stall by  $\sim 2deg$  to  $\sim 10.4deg$ .

A separate discussion is required for the pitching moment results, as experimental and numerical data show significantly different values in pitching moment coefficient. Experimental data show a more pronounced linear relation of the pitching moment curve up to stall condition with a higher slope  $C_{m\alpha_{exp}} = -0.014$  compared to a numerically obtained value of  $C_{m\alpha_{num}} = -0.0024$ . In addition, the significant variation of pitching moment between reference and corrected experimental data may be attributed to an insufficient correction with respect to support interference, as the presence of the sting has the most effect on pitching moment. At the same time, reference [1] and experimental data appear to be in agreement when predicting the aircraft to become longitudinally unstable at angle of attack  $\alpha > 8deg$ .

Data for side force, roll and yaw moment coefficients can only provide a qualitative insight on both the test and the aircraft: no reference data is available; experimental data is only corrected for blockage; and is of limited use when plotted against angle of attack. Yaw moment data in Figure. 8 (bottom left) show a drop in moment at  $\sim \alpha = 7deg$ , indicating an early localized onset of stall. Side force and



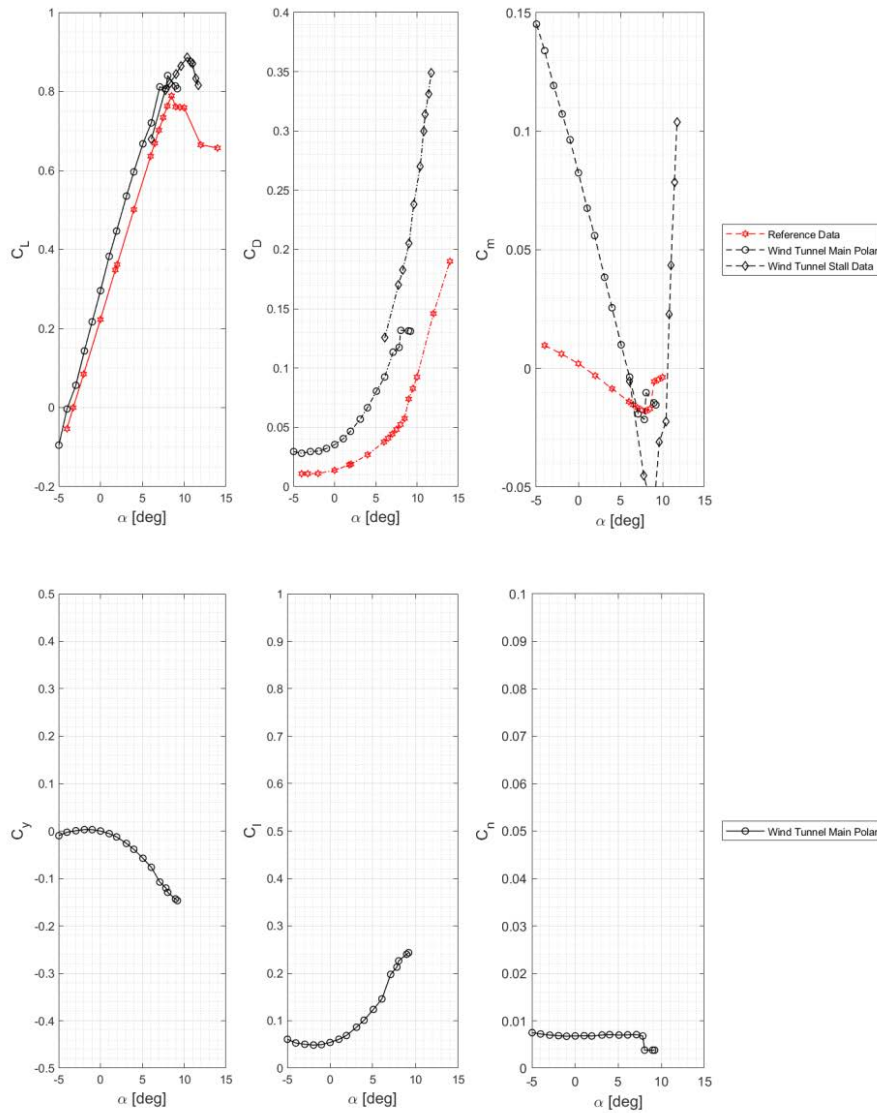


Figure 8 – Full Experimental Data

roll moment curves in Figure 8 (bottom left and bottom centre respectively) show unexpected varying coefficient values, suggesting that the model-to-sting alignment is slightly offset, since the sting only has been correctly aligned, as shown in Figure 2.

The progression of stall was evaluated qualitatively using thin wool tufts placed along the right wing section of the model. As shown in Figure 9 at wind velocity of 30m/s, flow initially separates at the outboard discontinuity at the trailing edge as early as  $\alpha = 7deg$ , and progressively moves upstream and inboard towards the wing root, until flow is separated over the entire wing. Flow over the fuselage does not appear to separate even at high angles of attack beyond stall. These qualitative results support those found in the reference data in Suwatanakul et al. [1], where a similar stall development was witnessed.

## 7. Future Work

Results presented in the paper are to be considered as preliminary, and future work will focus both on improving the “virtual wind tunnel” data as well as on expanding the test matrix.

Future numerical work will focus on enhancing the mesh analysis and on the application of other turbulence models to improve the quality of the numerical wind tunnel results and to estimate more accurate correction factors.

Future experimental work will focus on expanding the test matrix with the acquisition of data at a

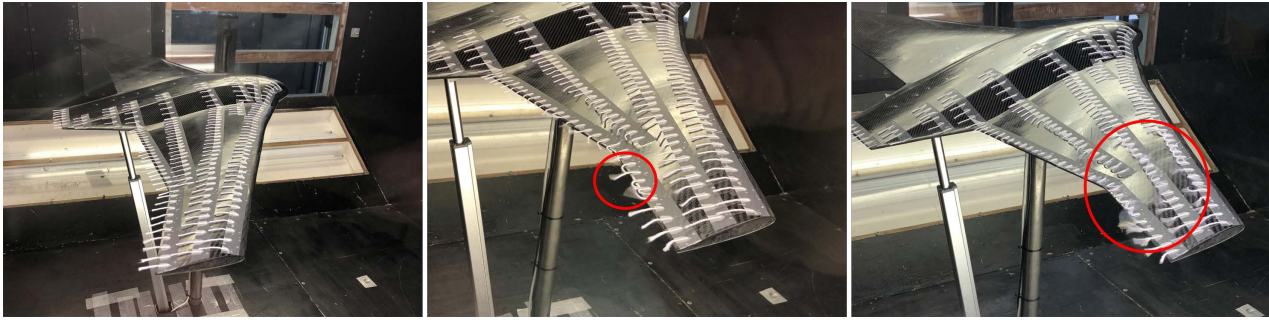


Figure 9 – Flow Separation Progression

range of yaw angles between 5deg and 15deg at 5deg intervals, in order to obtain more meaningful yaw and roll moment data. An experimental set-up for the estimation of support interference will also be investigated to complement the data obtained using the “virtual wind tunnel.”

From the perspective of the model set-up, the connection mechanics between the model and sting and the model and linear actuator will be re-evaluated to address the misalignment issues highlighted by the side force, roll and yaw moment data.

## 8. Conclusions

The paper presented the full work associated with the wind tunnel test campaign of a 37.5% scaled model of a blended-wing-body unmanned aerial vehicle. The test was conducted at the Large Low-Speed Wind Tunnel at the University of Bristol. The facility was replicated numerically in a “virtual wind tunnel” for preparatory work.

Wall and blockage corrections were calculated using classical approaches, and a total blockage of  $\varepsilon_t = 0.0027$  and a solid blockage of less than 5% was estimated for the 1.5m span model confirming that there was no need for wall interference correction and that blockage effects are nearly negligible. The “virtual wind tunnel” methodology was implemented to determine a-priori support interference and provide preliminary correction factors without the need of costly experimental work. Results obtained from the “virtual wind tunnel” and applied to numerical data indicated that sufficiently accurate correction factors for use in experimental work had been obtained.

The opening of the experimental domain highlighted good repeatability in the data acquisition, with accuracy in the range of  $\sim 1\%$  to  $\sim 1\%$ . Blockage corrections were confirmed to be nearly negligible. Support interference correction were shown to be sufficiently accurate for preliminary work, but in need of refinement to be fully acceptable.

The analysis of the aerodynamic performance indicated a higher maximum lift coefficient and angle of attack compared to reference numerical data, and a higher drag coefficient. The significantly higher drag coefficient may be attributed to both model surface finishing and the need to improve the mesh of the “virtual wind tunnel.”

Experimental pitching moment coefficient, which is strongly affected by the presence of the support, is significantly stronger compared to the numerically estimated value, and required further analysis, commencing with the improvement of the relevant correcting factors for support interference.

## 9. Contact Author Email Address

Corresponding Author: Raffaello Mariani [mailto: rmariani@kth.se](mailto:rmariani@kth.se)

## 10. Copyright Statement

The authors confirm that they, and/or their company or organization, hold copyright on all of the original material included in this paper. The authors also confirm that they have obtained permission, from the copyright holder of any third party material included in this paper, to publish it as part of their paper. The authors confirm that they give permission, or have obtained permission from the copyright holder of this paper, for the publication and distribution of this paper as part of the ICAS proceedings or as individual off-prints from the proceedings.

## Acknowledgments

The authors would like to acknowledge Selma Rahman and Mattias Olausson for providing high-quality CAD models of the aircraft, which were used in the numerical simulations and for manufacturing and Alessandro Porcarelli for his insightful comments on the numerical data. The authors would also like to thank Shuo Fu and Lei Feng at KTH for their contributing in developing the Simulink program for the actuator, and Xiao Liu and the technicians at the University of Bristol for the help in setting up the test campaign. The project has been funded by the KTH Integrated Transport Research Lab, KTH Industry Transformation Platform, the KTH Energy Platform, KTH XPRES, and KTH Excellenta Utnildningsmiljöer (KTH Excellence in Education).

## References

- [1] Suewatanakul S, Porcarelli A, Olsson A, Grimler H, Chiche A, Mariani R, Lindbergh G. Conceptual Design of a Hybrid Hydrogen Fuel Cell/Battery Blended-Wing-Body Unmanned Aerial Vehicle—An Overview. *Aerospace*, Vol. 9, No. 5, pp 275, 2021.
- [2] Guynn M D, Freeh J E and Olson E D. Evaluation of a Hydrogen Fuel Cell Powered Blended-Wing-Body Aircraft Concept for Reduced Noise Emission. *NASA/TM-2004-212989*
- [3] Bradley K R. A Sizing Methodology for the Conceptual Design of Blended-Wing-Body Transports. *NASA/CR-2000-213016*
- [4] Palermo M, Vos R. Experimental Aerodynamics of a 4.6%-scale Flying-V Subsonic Transport. *AIAA SciTech 2020 Forum*, Orlando, FL, USA, AIAA 2020-2228, pp 1-19, 2020.
- [5] Barlow J B, Rae W H Jr and Pope A. *Low-Speed Wind Tunnel Testing*. 3rd edition, John Wiley & Sons, 1999.
- [6] Haque A U, Asrar W, Omar A A, Sulaeman E and Ali M J S. Comparison of Data Correction Methods for Blockage Effects in Semispan Wing Model Testing. *EPJ Web of Conferences*, 2016.
- [7] Mouton S. Numerical Investigation of Model Support Interference in Subsonic and Transonic Wind Tunnels. *8th ONERA-DLR Aerospace Symposium*, Gotting, Germany, 2007.
- [8] Penela Guerrero L A. *Mechanical Design, Analysis, and Manufacturing of Wind Tunnel Model and Support Structure*. KTH Thesis, oai:DiVA.org:kth-310165, 2021.
- [9] Ghika S *Mechanical Design, Analysis, and Manufacturing of Wind Tunnel Model and Support Structure*. KTH Thesis, oai:DiVA.org:kth-305166, 2021.
- [10] Suewatanakul S. *Development of a Low Speed Wind Tunnel Test Campaign*. KTH Thesis, oai:DiVA.org:kth-310014, 2021.
- [11] Menter F, Kuntz M and Langtry R B. Ten Years of Industrial experience with the SST turbulence model. *Heat and Mass Transfer*, Vol. 4, No. 1, pp 625-632, 2003.
- [12] Spalart P R and Rumsey C L. Effective Inflow Conditions for Turbulence Models in Aerodynamic Calculations. *AIAA Journal*, Vol. 45, No. 10, pp. 2544-2553, 2007
- [13] Barlow B J, Rae W H Jr and Pope A. *Low-Speed Wind Tunnel Testing*. 3rd edition, John Wiley & Sons, 1999.
- [14] Horsten B J C. *Low-Speed Model Support Interference. Element of an Expert System*. Thesis, Technische Universiteit Delft, 2011, ISBN: 978-90-8891-294-8